Gauge-Including Atomic Orbital Proton Chemical Shifts of Strong Hydrogen Bonds: The Importance of Electron Correlation

Dewey H. Barich,[†] John B. Nicholas,*[,‡] and James F. Haw*[,§]

Department of Chemistry, Texas A&M University, P.O. Box 30012, College Station, Texas 77842-3012, Environmental Molecular Sciences Laboratory, Pacific Northwest National Laboratory, Richland, Washington 99352, and Loker Hydrocarbon Research Institute and Department of Chemistry, University of Southern California, University Park, Los Angeles, California 90089-1661

Received: November 9, 2000; In Final Form: January 29, 2001

The effects of electron correlation are often of little importance in theoretical ^{1}H NMR chemical shift calculations. Indeed, the differences between uncorrelated and correlated values are typically ca. 0.2 ppm or less for organic compounds. Here we demonstrate a very important case where this assumption breaks down; protons involved in strong hydrogen bonds. We found that the isotropic shifts calculated with the gauge-including atomic orbital (GIAO) approach at the RHF level overestimate the corresponding MP2 values by well over 1 ppm and commonly by 2 ppm. This is true for minimum energy geometries as well as for the transition states for proton transfer. In contrast, electron correlation effects are an order of magnitude smaller for the non-hydrogen-bonding protons in the structures we studied. The systems treated theoretically were FHF^-, $N_2H_7^+$, $H_3O_2^-$, the enol of 2,4-pentanedione, the monoanion of *cis*-maleic acid, and the monoanion of dimethylmalonic acid. Geometries were calculated at either the MP2/6-311++G** or MP2/aug-cc-pVTZ level of theory. The donor−acceptor distances and other geometric parameters for most structures satisfy the standard criteria for "strong" hydrogen bonds. A notable exception is the minimum energy structure for the enol of 2,4-pentanedione, which is better classified as a "moderate" hydrogen bond on the basis of both geometric and chemical shift criteria. The effect of electron correlation on the ^{1}H chemical shift in the latter case was the smallest of any structure we considered.

Introduction

Short, strong hydrogen bonds are under intense investigation.[1−13] The clearest examples of such bonds are from gas-phase studies. In solution, considerations for the formation of such bonds include the pK_as of the proton donors and acceptors, the charges of the donors and acceptors, and the dielectric constant.[1] Cleland and Krevoy have suggested that strong hydrogen bonds play an important role in enzyme catalysis.[8] This has led to a lively debate[14−17] and has also prompted a reexamination of potential surfaces for proton transfer, the relative contributions of electrostatic and covalent bonding, and the origin and significance of spectroscopic signatures of hydrogen bonding.[1,18] One of the most characteristic traits of strong hydrogen bonds is their ^{1}H NMR isotropic chemical shift. Protons in hydrogen bonds resonate downfield of essentially all other typical organic functional groups, and values in the range 18−22 ppm are observed for the protons central to many of the strongest hydrogen bonds.[19,20]

While the existence and significance of short, strong hydrogen bonds in enzymic catalysis is controversial,[1,14,16,18] it is certain that such bonding is important for many reactants adsorbed on inorganic solid acid catalysts.[21,22] For example, we have observed large downfield ^{1}H isotropic chemical shifts for the Brønsted acid site hydrogens of zeolite catalysts upon adsorption of ketones or other basic hydrogen bond acceptors. Theoretical studies modeling the experimental observations verify the central importance of hydrogen bonding to these systems. It is desirable to perform chemical shift calculations to obtain a direct link between NMR experiments and these theoretical predictions of molecular structure. NMR shifts can be calculated with a variety of theoretical methods; we prefer to use the gauge-including atomic orbitals (GIAO) formalism.[23,24] GIAO calculations can be done at the RHF level (GIAO-RHF) or with the inclusion of electron correlation via second-order perturbation theory (GIAO-MP2).[25] GIAO-MP2 calculations are much more computationally demanding than GIAO-RHF calculations with the same basis set. Considering that many hydrogen-bonded systems of interest are large from a computational point of view, one would hope to be able to neglect electron correlation. Indeed, a common assumption[3] is that electron correlation contributions to ^{1}H shifts are negligible (0.2 ppm or less), except in unusual cases such as fluorine-containing molecules,[26] and can thus be ignored.

To lay a foundation for chemical shift calculations of hydrogen-bonded complexes on solid acids, we sought to better understand the significance of correlation in proton shift calculations by carrying out theoretical studies of a set of more conventional hydrogen bonding systems. The systems we studied included, for generality, anion, cation, and neutral cases as well as O, N, and F as the donor−acceptor atoms. Our structural calculations used both correlated methods and large basis sets. Both of these traits have recently been shown to be needed for reliable structural determinations for hydrogen-bonded systems.[27] Geometries were calculated at the MP2/aug-cc-pVTZ level of theory for FHF^-, $N_2H_7^+$, $H_3O_2^-$, or the MP2/6-311++G** level for the enol form of 2,4-pentanedione, the

[†] Texas A&M University.
[‡] Pacific Northwest National Laboratory.
[§] University of Southern California.

10.1021/jp004118d CCC: $20.00
Published on Web 04/17/2001

TABLE 1: Parameters Used To Classify Hydrogen Bonds

property	bond classification		
	strong	moderate	weak
$R_{H\cdots B}$, Å	1.2−1.5	1.5−2.2	2.2−3.2
$R_{A\cdots B}$, Å	2.2−2.5	2.5−3.2	3.2−4.0
∠AHB, deg	175−180	130−180	90−150
bond energy, kcal/mol	14−40	4−15	<4
^{1}H shift, ppm	14−22	<14	

monoanion of *cis*-maleic acid, and the monanion of dimethylmalonic acid. Minimum energy geometries and transition states for proton transfer were calculated. Chemical shift calculations were performed on all geometries at both GIAO-RHF and GIAO-MP2 with four different basis sets. Significantly, we find that electron correlation has a large effect on the calculated ^{1}H isotropic shift for hydrogens involved in strong hydrogen bonds, and GIAO-RHF values overestimate the GIAO-MP2 results by up to 2.1 ppm. In contrast, the electron correlation contribution was 0.2 ppm or less for protons not involved in hydrogen bonding, in agreement with previous findings.

The availability of GIAO-MP2 ^{1}H shifts for MP2 geometries also allows us to assess the usefulness of the ^{1}H shift criterion for classification of hydrogen bonds. Table 1 summarizes one popular scheme, from Jeffrey's book,[28] for the classification of hydrogen bonds based on structure, energy, or ^{1}H shift. For example, Table 1 classifies "strong" hydrogen bonds as having donor−acceptor distances (R_{A-B}) of 2.5 Å or less and ^{1}H shifts of 14 ppm or more. "Moderate" hydrogen bonds are proposed to have longer donor−acceptor distances and lower ^{1}H shifts. While the demarcation between "strong" and "moderate" is necessarily arbitrary, we find that the $R_{A\cdots B}$ and ^{1}H shift criteria in Table 1 result in *consistent* classifications for all but one of the structures we examined.

Methods

Initial geometry optimizations were done with density functional theory, the B3LYP[29,30] exchange-correlation functional, and the 6-31++G**[31] basis set. The B3LYP/6-31++G** level of theory was used to obtain the zero-point and thermal energies. Frequency calculations were used to identify the optimized geometries as ground or transition states. The thermal energies and frequency calculations used a temperature of 298.15 K. The geometries of the enol of 2,4-pentanedione, hydrogen maleate, and hydrogen dimethyl malonate were then optimized at the MP2[32] level with the 6-311++G** basis set.[33] The smaller molecules studied, FHF^-, $N_2H_7^+$, and $O_2H_3^-$, were also optimized at the MP2 level, but for these we were able to use Dunning's aug-cc-pVTZ[34] basis set, which is considerably more complete than 6-311++G**. The core electrons were frozen in all MP2 optimizations and frequency calculations. All optimizations and frequency calculations were done with Gaussian94.[35]

We then calculated the chemical shift tensors for all MP2-optimized structures at the RHF and MP2[25] levels with the gauge-including atomic orbital (GIAO) formalism.[23,24] The basis sets used included dzp {5111/311/1}, tzp {51111/311/1}, and tzplarge {511111/411/1}.[36] In addition, we also used the tz2p (51111/311/11) basis set on the three atoms involved in the hydrogen bond (i.e., A−H···B), with tzp on all remaining atoms.[36] For simplicity, the tz2p/tzp scheme is designated tz2p throughout. We used ACES II[37] for all the NMR calculations.

The theoretical chemical shielding tensors were symmetrized and diagonalized in order to yield principal components.[38] The values reported are referenced to the ^{1}H isotropic chemical shift of hydrogen in tetramethylsilane (TMS), calculated at the same level of theory, thus $\delta_{calc} = \sigma_{TMS} - \sigma_{calc}$. The absolute shieldings of ^{1}H in TMS are reported in Table 2. The isotropic chemical shift is the average of the three principal components, which are sorted so that $\delta_{11} \geq \delta_{22} \geq \delta_{33}$. Thus,

$$\delta_{iso} = {}^1/_3(\delta_{11} + \delta_{22} + \delta_{33})$$

The asymmetry factor (η) and chemical shift anisotropy (CSA) are defined by the following equations as presented in a compilation of chemical shift anisotropy data.[39]

For $|\delta_{11} - \delta_{iso}| \geq |\delta_{33} - \delta_{iso}|$,

$$CSA = {}^3/_2(\delta_{11} - \delta_{iso})$$

$$\eta = (\delta_{22} - \delta_{33})/(\delta_{11} - \delta_{iso})$$

For $|\delta_{11} - \delta_{iso}| \leq |\delta_{33} - \delta_{iso}|$,

$$CSA = {}^3/_2(\delta_{33} - \delta_{iso})$$

$$\eta = (\delta_{22} - \delta_{11})/(\delta_{33} - \delta_{iso})$$

TABLE 2: Absolute Chemical Shieldings (in ppm) for ^{1}H in TMS

basis for shifts	MP2/6-311++G** Opt		MP2/aug-cc-pVTZ Opt	
	GIAO-RHF	GIAO-MP2	GIAO-RHF	GIAO-MP2
tz2p	32.069	31.707	32.189	31.825
tzplarge	32.201	31.896	32.322	32.015
tzp	32.184	31.883	32.306	32.003
dzp	32.002	31.643	32.121	31.760

TABLE 3: Selected Hydrogen Bond Structural Parameters

molecule	R_{A-H}, Å	R_{B-H}, Å	R_{A-B}, Å	∠AHB, deg
1	1.144	1.144	2.288	180.0
2	1.118	1.578	2.697	180.0
2ts	1.300	1.300	2.600	180.0
3	1.112	1.365	2.477	177.9
3ts	1.221	1.221	2.443	179.8
4	0.998	1.631	2.547	150.5
4ts	1.197	1.197	2.354	159.3
5	1.107	1.299	2.406	179.3
5ts	1.193	1.193	2.385	179.8
6	1.104	1.307	2.390	165.0
6ts	1.194	1.194	2.369	165.8

Results

Geometries. Hydrogen bonds are commonly classified by several geometric parameters, R_{A-H}, R_{B-H}, R_{A-B}, and ∠AHB. R_{A-B} is probably the most useful structural parameter in studies of hydrogen bonding; it has been determined with very high accuracy from a wealth of crystal structures. The other three parameters are more challenging to obtain experimentally due to the difficulty of locating hydrogens on electron density maps. The theoretical values of the four parameters for all of the species studied are collected in Table 3. Most of the parameters reported are within the range of typical strong hydrogen bonds.[28] Each of the structures is discussed in detail below.

We start with the bifluoride anion, FHF^-, a commonly studied example of a strong hydrogen bond. Figure 1 reports the MP2/aug-cc-pVTZ optimized structure of FHF^- (**1**). Crystal structure determinations of R_{A-B} (in this case the F···F distance) range from 2.25 Å[40] to 2.29 Å,[41] depending on the counterion present. We calculate an F···F distance of 2.288 Å, well within the range of experimental values, and similar to a value of 2.283 Å previously obtained at the MP2/6-311++G(2d,2p) level.[42] The

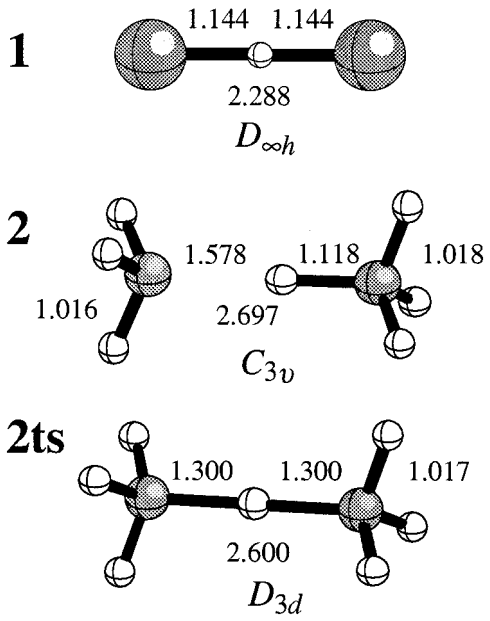

Figure 1. MP2/aug-cc-pVTZ optimized geometries of (a) the FHF^- anion, (b) the ground state of $N_2H_7^+$, and (c) the transition state of $N_2H_7^+$. Selected bond lengths (Å) and angles (deg) are shown.

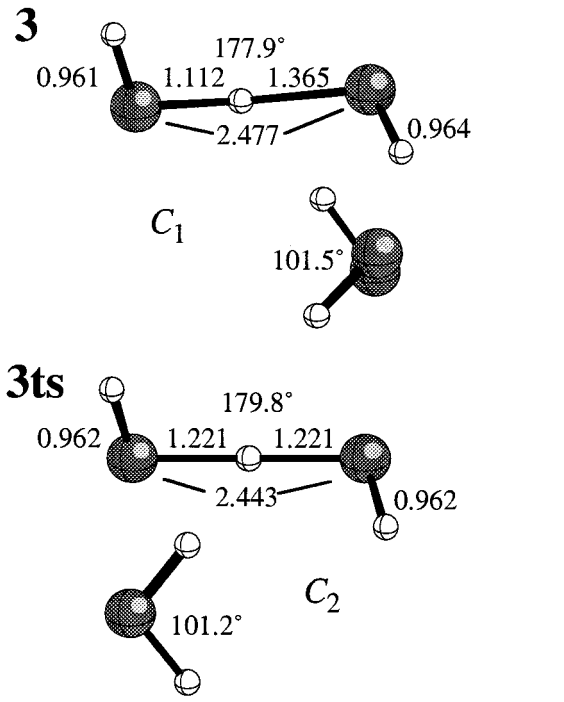

Figure 2. MP2/aug-cc-pVTZ optimized geometries of (a) the $O_2H_3^-$ anion, (b) the $O_2H_3^-$ anion transition state. Selected bond lengths (Å) and angles (deg) are shown, as are side views of the anions to show the torsional angle in each molecule.

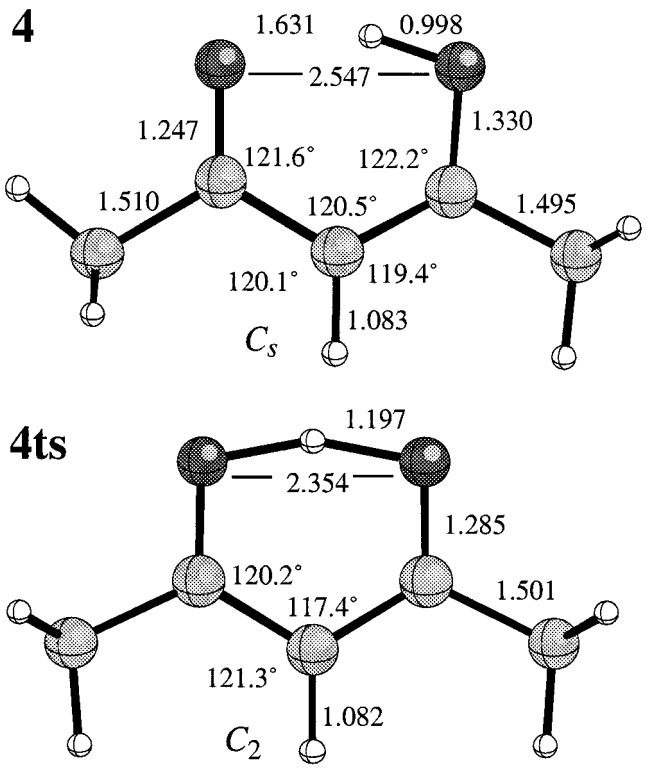

Figure 3. MP2/6-311++G** optimized geometries of (a) the 2,4-pentanedione anion and (b) the transition state of 2,4-pentanedione. Selected bond lengths (Å) and angles (deg) are shown.

hydrogen atom is located exactly between the fluorines in this linear anion, thus the AHB angle is 180.0°.

Figure 1 reports the MP2/aug-cc-pVTZ optimized geometries for the ground and transition state for proton transfer along the hydrogen bond coordinate for $N_2H_7^+$ (**2**), a simplified theoretical model of a "proton sponge".[28] The minimum energy geometry can be viewed as an ammonium cation hydrogen bonded to an ammonia molecule. The minimum energy geometry has an R_{A-B} (N···N) of 2.697 Å (cf. 2.816 Å at MP2/6-311++G(2d,2p) in ref 43), with $R_{A-H} = 1.578$ Å and $R_{H-B} = 1.118$ Å. The N···N distance here is in near-quantitative agreement with a recent crystal structure determination of the $N_2H_7^+$ cation in the monoammonia adduct of ammonium iodide,[44] in which it is 2.695 Å. The R_{A-B} values for both **2** and **2ts** are in the range of the N···N distances in crystal structures of protonated 1,8-bis(dimethylamine) naphthalene, an established strong hydrogen bond.[28] The transition state for proton transfer (**2ts**) is symmetric about the central hydrogen, having R_{A-H} and R_{H-B} of 1.300 Å and an R_{A-B} distance of 2.600 Å. As found in other investigations of hydrogen bonding, R_{A-B} is shorter in the transition state than in the minimum energy geometry. In both **2** and **2ts** ∠AHB is 180°.

Figure 2 reports the structures of the minimum energy geometry of $O_2H_3^-$ (**3**) and the transition state (**3ts**) for hydrogen exchange. In the minimum energy geometry R_{A-H} and R_{B-H} are 1.112 and 1.365 Å, respectively, whereas ∠AHB is 177.9°. The O···O distance contracts from 2.477 Å in the minimum energy geometry to 2.443 Å in the transition state. In the transition state ∠AHB becomes 179.8°, closer to 180°.

The minimum energy and transition state geometries for the enol of 2,4-pentanedione (**4** and **4ts**) are shown in Figure 3. The minimum energy geometry has two very different H−O bond lengths, $R_{A-H} = 0.998$ Å and $R_{B-H} = 1.631$ Å. This latter value is more consistent with a moderate hydrogen bond, as is the AHB angle of 150.5°. R_{A-B} is 2.547 Å, in reasonable agreement with a gas-phase electron diffraction value of 2.512 Å.[45] This O···O distance is significantly longer than those in the other O−H−O hydrogen bonds considered in this investigation. While the hydrogen bond in **4** is undoubtedly constrained by its intramolecular nature, hydrogen bonds in neutral systems tend to be longer (and weaker) than in anions. The geometric parameters for **4** are consistent with classifications of moderate hydrogen bonds, while those for all other structures considered here (both ground and transition states) are consistent with strong hydrogen bonds (see below). In the transition state ∠AHB increases by almost 9°.

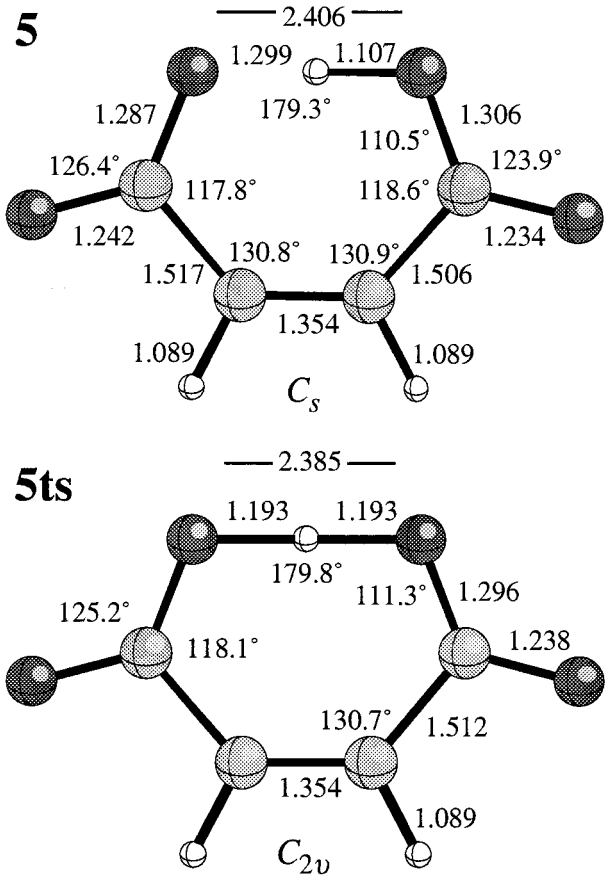

Figure 4. MP2/6-311++G** optimized geometries of (a) the hydrogen maleate anion and (b) the transition state of the hydrogen maleate anion. Selected bond lengths (Å) and angles (deg) are shown.

The minimum energy geometry of the monoanion of *cis*-maleic acid (hydrogen maleate) **5** and the corresponding transition state structure **5ts** are shown in Figure 4. The MP2/6-31+G(d,p) geometry of the ground state was reported in a recent study.[4] The earlier study reports an O···O distance of 2.49 Å and an ∠AHB of 172.2°. The larger basis set used in this work results in a significantly shorter O···O distance (2.406 Å) and a larger ∠AHB (179.3°). A double-well energetic potential is reflected in R_{A-H} = 1.107 Å and R_{B-H} = 1.299 Å. In the transition state R_{A-B} shortens to 2.385 Å and $R_{A-H} = R_{B-H}$ = 1.193 Å. ∠AHB is 179.8° in the transition state, essentially unchanged from the minimum energy geometry.

The structures of the ground and transition state of the hydrogen dimethylmalonate anion (**6** and **6ts**, respectively) are reported in Figure 5. In the ground state R_{H-A} is 1.104 Å, R_{B-H} is 1.307 Å, R_{A-B} is 2.390 Å, and ∠AHB is 164.9°. In the transition state the AHB angle is 165.8°, whereas R_{A-B} is 2.369 Å. R_{H-A} and R_{H-B} are both 1.194 Å. The geometric parameters for the hydrogen bonds in **6** and **6ts** (Table 3) are very similar to those in the corresponding structures **5** and **5ts**, despite the differing carbon backbones.

Energetics. The electronic, zero-point, and thermal energies for all species are reported in Table 4. Also included are energies and enthalpies for each molecule reported relative to the minimum energy state. As would be implied from our earlier discussion, five of the species (**2**−**6**) have transition states for proton transfer, and thus are symmetric double-well potentials if we consider only the electronic energies. The barriers to proton transfer are small; with the exception of **4**, the transition state is less than 0.8 kcal/mol higher in energy than the ground state. The zero-point and thermal energies behave oppositely, being

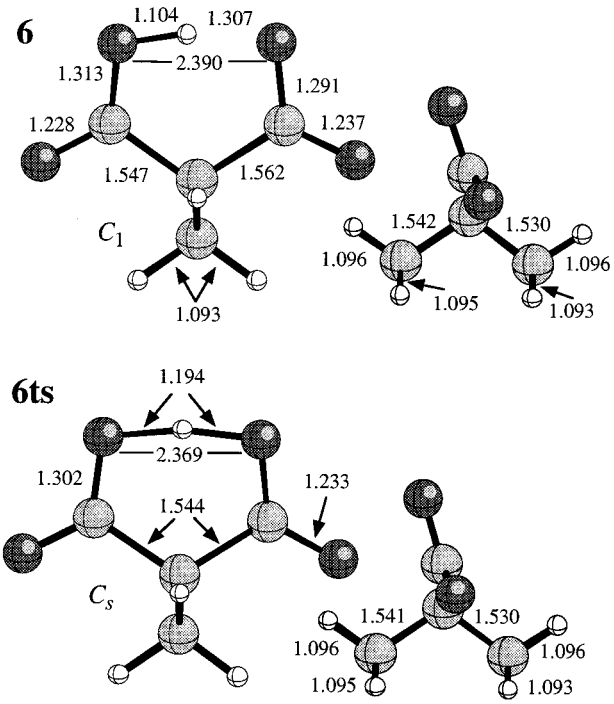

Figure 5. MP2/6-311++G** optimized geometries of (a) the hydrogen dimethylmalonate anion, (b) the transition state of the hydrogen dimethylmalonate anion. Selected bond lengths (Å) and angles (deg) are shown. Side views of the anions are provided for clarity.

≈1.0 kcal/mol lower for the transition states than the ground states. Thus, when we consider enthalpies, we find that only **4** has a barrier to proton transfer, although it is very slight (0.07 kcal/mol). We can clearly classify **4** as a "low barrier" hydrogen bond. Molecules **2** and **3**−**6** are all single-well potentials, with the transition-state geometry being lower in enthalpy than the ground-state geometry by ≈1.0 kcal/mol. It would thus be inappropriate to use the "low barrier" terminology for the hydrogen bonds in these molecules. Consideration of the enthalpies is clearly important to the classification of hydrogen bonds, especially when the differences in the calculated chemical shift between the ground and transition states can be large (see below).

Chemical Shifts. One of the most distinctive characteristics of the hydrogens involved in strong hydrogen bonds is their isotropic chemical shift. It is important to be aware of how correlation affects both the chemical *shielding* and the chemical *shift*. Whereas theoretical predictions of the chemical shielding are obtained directly from the calculations and are referenced to the bare nucleus, the chemical shift is the difference between the shielding of the selected nucleus in the molecule under study and that in a reference molecule, which in this case is ^{1}H in TMS. Theoretical shieldings are generally in poorer agreement with experimental values (which have to be interpolated from experimental shifts) than are theoretical shifts, as the errors that enter into the calculation (caused by lack of electron correlation, insufficient basis sets, etc.) tend to cancel in the determination of chemical shifts.

For the hydrogen-bonded hydrogens in the molecules studied here we find the difference between the GIAO-RHF and GIAO-MP2 shieldings calculated with the dzp basis set to be as high as 1.18. The differences were 1.31, 1.31, and 1.29 ppm for the tzp, tzplarge, and tz2p basis sets. In all of these cases, the GIAO-MP2 values were more positive than the GIAO-RHF values. For all four basis sets used this difference is greater than has previously been suggested for correlation effects for ^{1}H chemical

TABLE 4: Electronic, Zero-Point, and Thermal Energies for Molecules 1−6ts

species	basis set for MP2 opt	MP2(fc), hartrees	ZPE,[a] hartrees	thermal,[a] hartrees	ΔE kcal/mol	ΔH,[b] kcal/mol
1	aug-cc-pVTZ	200.157 783	0.010 592	0.002 537	0.00	0.00
2	aug-cc-pVTZ	113.299 265	0.086 114	0.005 019	0.00	0.00
2ts	aug-cc-pVTZ	113.298 112	0.083 678	0.004 724	0.72	0.99
3	aug-cc-pVTZ	152.074 583	0.030 381	0.004 255	0.00	0.00
3ts	aug-cc-pVTZ	152.074 451	0.028 952	0.003 904	0.08	1.03
4	6-311++G**	344.937 928	0.122 656	0.007 869	0.00	0.00
4ts	6-311++G**	344.933 705	0.118 940	0.007 473	2.65	0.07
5	6-311++G**	454.213 064	0.067 289	0.006 892	0.00	0.00
5ts	6-311++G**	454.212 991	0.065 634	0.006 590	0.05	1.18
6	6-311++G**	494.630 978	0.117 634	0.009 082	0.00	0.00
6ts	6-311++G**	494.630 901	0.116 291	0.008 746	0.05	1.01

[a] Zero-point and thermal energies were determined at B3LYP/6-31++G**//B3LYP/6-31++G**. Thermal energies determined at 298.15 K. [b] Enthapies were determined at the sum of the electronic, zero-point, and thermal energies.

TABLE 5: GIAO-RHF and GIAO-MP2 Calculated ^{1}H Chemical Shift Tensors

		GIAO-MP2						GIAO-RHF					
	NMR basis	δ_{iso}, ppm	δ_{11}, ppm	δ_{22}, ppm	δ_{33}, ppm	CSA, ppm	η	δ_{iso}, ppm	δ_{11}, ppm	δ_{22}, ppm	δ_{33}, ppm	CSA, ppm	η
1	tz2p	18.8	37.3	37.3	18.1	55.5	0.00	20.5	39.0	39.0	16.6	55.6	0.00
	tzplarge	18.0	35.9	35.9	17.9	53.8	0.00	19.7	37.7	37.7	16.3	54.0	0.00
	tzp	18.4	36.5	36.5	17.9	54.3	0.00	19.9	38.0	38.0	16.4	54.4	0.00
	dzp	18.5	36.7	36.7	18.0	54.8	0.00	19.9	38.1	38.1	16.5	54.6	0.00
2	tz2p	18.5	33.3	33.3	11.2	44.5	0.00	19.4	34.1	34.1	10.2	44.3	0.00
	tzplarge	18.3	32.9	32.9	11.0	43.9	0.00	19.1	33.7	33.7	10.2	43.9	0.00
	tzp	18.0	32.5	32.5	11.0	43.5	0.00	18.9	33.4	33.4	10.2	43.6	0.00
	dzp	17.3	31.3	31.3	10.9	42.3	0.00	18.2	32.4	32.4	10.1	42.5	0.00
2ts	tz2p	23.6	40.7	40.7	10.7	51.4	0.00	25.1	42.3	42.3	9.5	51.8	0.00
	tzplarge	23.3	40.2	40.2	10.5	50.7	0.00	24.7	41.8	41.8	9.4	51.2	0.00
	tzp	23.0	39.8	39.8	10.5	50.3	0.00	24.5	41.5	41.5	9.5	51.0	0.00
	dzp	22.0	38.2	38.2	10.5	48.7	0.00	23.6	40.1	40.1	9.4	49.6	0.00
3	tz2p	17.4	35.4	34.7	17.8	52.9	0.02	19.2	37.2	36.5	16.0	53.0	0.02
	tzplarge	16.7	34.3	33.4	17.6	51.5	0.03	18.5	36.1	35.4	16.0	51.7	0.02
	tzp	16.6	34.0	33.2	17.5	51.1	0.02	18.3	35.8	35.2	16.0	51.5	0.02
	dzp	16.1	33.1	32.6	17.4	50.3	0.02	17.8	34.9	34.4	16.0	50.6	0.02
3ts	tz2p	19.2	37.6	37.6	17.7	55.3	0.00	21.2	39.7	39.7	15.9	55.6	0.00
	tzplarge	18.5	36.5	36.4	17.5	54.0	0.00	20.5	38.6	38.5	15.7	54.3	0.00
	tzp	18.3	36.2	36.1	17.4	53.5	0.00	20.3	38.3	38.3	15.8	54.1	0.00
	dzp	17.8	35.4	35.2	17.3	52.6	0.01	19.7	37.5	37.3	15.8	53.1	0.00
4	tz2p	14.3	27.5	16.3	0.8	22.8	0.74	15.2	28.9	17.4	0.7	23.9	0.72
	tzplarge	14.2	26.9	15.7	0.1	21.4	0.79	14.9	28.3	16.7	0.1	22.6	0.77
	tzp	14.1	27.1	15.5	0.3	21.6	0.81	14.8	28.4	16.5	0.4	22.8	0.78
	dzp	13.6	26.7	15.1	1.1	22.0	0.80	14.2	27.8	16.0	1.1	23.0	0.77
4ts	tz2p	23.6	40.4	28.8	1.7	32.8	0.53	25.7	43.7	31.5	2.0	35.6	0.51
	tzplarge	23.4	39.6	27.9	2.7	31.1	0.56	25.4	43.0	30.5	2.7	34.0	0.55
	tzp	23.3	39.9	27.5	2.4	31.3	0.59	25.3	43.2	30.2	2.5	34.2	0.57
	dzp	22.5	39.2	26.7	1.5	31.4	0.60	24.3	42.1	29.2	1.5	34.2	0.57
5	tz2p	21.5	37.0	29.5	2.1	35.3	0.32	23.3	39.4	32.3	1.9	37.7	0.28
	tzplarge	21.3	36.4	28.7	1.2	33.7	0.34	23.0	38.9	31.3	1.2	36.3	0.31
	tzp	21.2	36.5	28.4	1.4	33.9	0.35	22.8	38.8	31.2	1.5	36.5	0.32
	dzp	20.7	36.1	28.2	2.1	34.2	0.35	22.3	38.3	30.8	2.1	36.7	0.31
5ts	tz2p	22.6	38.7	31.2	2.0	36.9	0.31	24.6	41.4	34.2	1.7	39.5	0.27
	tzplarge	22.5	38.1	30.3	1.0	35.3	0.33	24.4	40.8	33.2	1.0	38.0	0.30
	tzp	22.3	38.2	30.1	1.3	35.4	0.34	24.2	40.8	33.1	1.3	38.2	0.30
	dzp	21.8	37.8	29.7	2.0	35.7	0.34	23.6	40.2	32.6	2.0	38.4	0.30
6	tzp.tz2p	21.3	38.2	26.4	0.8	33.1	0.53	23.1	40.2	29.4	0.4	35.2	0.46
	tzplarge	21.0	37.5	25.6	0.2	31.8	0.56	22.7	39.6	28.5	0.1	33.9	0.49
	tzp	20.9	37.8	25.1	0.3	31.7	0.60	22.6	39.8	28.1	0.0	33.9	0.52
	dzp	20.2	37.0	24.5	0.7	31.5	0.59	21.9	38.8	27.5	0.5	33.7	0.50
6ts	tz2p	22.5	40.1	28.1	0.8	34.9	0.51	23.3	40.5	29.6	0.4	35.5	0.46
	tzplarge	22.2	39.4	27.4	0.2	33.6	0.54	22.6	38.8	28.6	0.4	33.3	0.46
	tzp	22.1	39.7	26.9	0.2	33.5	0.58	22.4	39.1	27.8	0.2	33.2	0.51
	dzp	21.4	38.8	26.1	0.7	33.2	0.57	21.5	38.1	27.1	0.5	33.1	0.50

shieldings (0.2 ppm).[26] In contrast to these large differences, we find that inclusion of electron correlation changes the ^{1}H chemical shieldings in TMS by only about 0.4 ppm (Table 2). For TMS the GIAO-MP2 values are predicted to be more negative than the GIAO-RHF results. Thus, our calculated shifts for the proton involved in the hydrogen bond have a correlation contribution of up to 2.12 ppm (Table 5). The average difference between the GIAO-MP2/dzp and GIAO-RHF/dzp shifts for the hydrogen-bonded hydrogens is 1.54 ± 0.39 ppm. As the quality of the basis set is improved, the difference between chemical shifts calculated at the GIAO-MP2 and GIAO-RHF levels generally increases by several tenths of a part per million (1.62 ± 0.42 ppm, 1.62 ± 0.45 ppm, 1.68 ± 0.44 ppm with the tzp, tzplarge, and tz2p basis sets, respectively). Thus, this difference does not appear to be due to a deficiency in the basis set and would not likely diminish if even larger basis sets were used.

In contrast, on average the GIAO-RHF/dzp shifts of these other protons were only 0.16 ± 0.18 ppm more positive than the GIAO-MP2/dzp shifts. The larger basis sets yield values (in ppm) of 0.18 ± 0.18, 0.22 ± 0.19, and 0.22 ± 0.19 for the tzp, tzplarge, and tz2p basis sets, respectively. However, for this group of hydrogens the GIAO-RHF shielding is not always more positive than the GIAO-MP2 shielding. The effect of correlation on the other ^{1}H isotropic shieldings in these molecules is such that the average absolute difference between GIAO-MP2 and GIAO-RHF values is only 0.20 ± 0.12 ppm with the dzp basis set. For the larger basis sets the values are 0.21 ± 0.14, 0.24 ± 0.16, and 0.24 ± 0.15 for the tzp, tzplarge, and tz2p basis sets, respectively. It thus appears that calculated NMR shieldings for hydrogens involved in strong hydrogen bonds are much more sensitive to electron correlation than those of hydrogens in more conventional environments. In the following we will focus on the tz2p data because this basis set is the highest quality that we have used.

We again begin with FHF^- (**1**). Well-characterized as a strong hydrogen bond in the gas phase, the calculated isotropic chemical shift of 18.8 ppm for the hydrogen is consistent with a strong hydrogen bond. The GIAO-RHF isotropic shift is 1.7 ppm downfield of the GIAO-MP2 result. The experimentally determined isotropic chemical shift of a single crystal of KHF_2 is 21.1 ppm.[41] That work also reports the chemical shift tensor, for which $\delta_{11} = 39.7$, $\delta_{22} = 32.4$, and $\delta_{33} = -8.8$ ppm. The symmetry of the calculated anion requires that its chemical shift tensor be axially symmetric (two principal components must be identical), but this was not observed in the single crystal study. The packing of the crystal could easily impose a symmetry upon the anion lower than that in the gas phase. The agreement between theoretical and experimental results is nevertheless reasonable. We have seen in other work that the calculated chemical shift tensor principal components often bracket the experimental principal components, possibly due to thermal motion in the experimental determinations.[46] We find the same here and thus expect our value of −55.5 ppm to overestimate the measured chemical shift anisotropy of −44.9 ppm. Here we find differences between corresponding principal components ranging from 2.3 to 9.3 ppm. In absolute terms, this rivals the accuracy of a number of ^{13}C chemical shift tensor calculations with the GIAO-MP2 approach.[38,46,47] We should note that NMR tensor values, and thus chemical shift anisotropies, are also known to be sensitive to the effects of neighboring atoms, which are ignored in the current work.[50,51]

While structurally consistent with a moderate hydrogen bond, the proton in the ground state of $N_2H_7^+$ (**2**) has an isotropic chemical shift of 18.5 ppm, typical of a strong hydrogen bond. The chemical shift of the same proton in the transition state (**2ts**) is very far downfield at 23.6 ppm. The Boltzmann-weighted (based on the enthalpies) GIAO-MP2 chemical shift is 23.1 ppm. For **2** the GIAO-RHF/tz2p shift overestimates the GIAO-MP2 result by 0.9 ppm, one of the smallest discrepancies we found. However, this difference increases to 1.5 ppm in the transition state.

For $O_2H_3^-$ (**3**) the GIAO-MP2 isotropic shifts of 17.4 and 19.2 ppm for the ground (**3**) and transition states (**3ts**) suggest strong hydrogen bonds, consistent with the O···O distances. The Boltzmann-weighted chemical shift is 18.8 ppm. The difference of only 1.8 ppm between the ^{1}H NMR of the ground and transition states is consistent with the similarity of the geometries. Here again the GIAO-RHF shifts overestimate the corresponding GIAO-MP2 results by 1.8 and 2.0 ppm, respectively.

Of the molecules we have studied, the enol form of the 2,4-pentanedione anion (**4**) shows the most dramatic change in the calculated ^{1}H NMR between the ground and transition states. The GIAO-MP2 isotropic chemical shifts are 14.3 ppm for the minimum energy structure and 23.6 ppm for the transition state. The isotropic chemical shift of the ground state is typical of a moderate hydrogen bond. In contrast, the chemical shift of the transition state clearly indicates a strong hydrogen bond. The Boltzmann-weighted average chemical shift is 17.2 ppm, which compares to the experimental solution phase chemical shift of 15.40 ppm.[48] It is possible that taking a temperature-weighted average over more points along the enthalpy surface for proton movement might improve the agreement with experiment. The large change in chemical shift between the ground and transition states is consistent with the large changes in R_{A-H} and R_{A-B}.

The calculated GIAO-MP2 isotropic chemical shift (21.5 ppm) of the hydrogen maleate anion (**5**) agrees reasonably well with the experimental value of 20.9 ppm. The Boltzmann-weighted chemical shift is 22.3 ppm. The chemical shift tensor for the transition state is very similar to that of the ground state. The isotropic chemical shift moves only 1.1 ppm downfield of that in the ground state. As with **1**, the chemical shift tensor agrees reasonably well with the measured tensor values, which in this case are δ_{11}=32.5, δ_{22}=29.6, and δ_{33}=0.7 ppm.

The hydrogen dimethyl malonate anion (**6**), like the hydrogen maleate above, shows little difference in chemical shift between the ground and transition states. This is consistent with the small difference in geometry between the two states. The minimum energy geometry has an isotropic chemical shift of 21.3 ppm whereas the transition state has an isotropic chemical shift of 22.5 ppm. The Boltzmann averaged GAIO-MP2 value is 22.2 ppm. The calculated NMR values indicate that both states correspond to strong hydrogen bonds. Like all the other cases studied here, the isotropic chemical shift for the transition state is farther downfield than the minimum.

Tensor Orientation. An important benefit of chemical shift calculations is that they provide the orientation of the chemical shift tensor. The tensor orientations for several of the molecules here are sufficiently simple that they can be described without visual representation. For example in **1**, **2**, and **2ts** the hydrogen-bonded hydrogen lies on an axis that has at least C_3 symmetry, making the tensor for that proton axially symmetric. As a result, one component will lie along the symmetry axis; the other two (which are equal in magnitude) will lie in a plane that is perpendicular to that axis. Figure 6 reports the chemical shift tensor orientation for **4** and **4ts**. In each case there is a plane of symmetry coincident with the page, thus requiring that one of the three principal components lie perpendicular to the plane of the page. In both cases this is δ_{11}. In Figure 6a the angle between δ_{22} and the H−O bond is 82.5°. In Figure 6b, the angle between δ_{33} and the nearest H−O bond is 10.4°. The tensor orientations for the hydrogen-bonded hydrogens in **5**, **5ts**, **6**, and **6ts** are qualitatively similar to those in **4** and **4ts**.

Discussion

We will now discuss the differences in geometrical features of the ground and transition states of the molecules studied and the relation to their calculated chemical shifts. With the exception of the ground state for **4**, the geometries for all species studied here are consistent with the expected structural parameters of strong hydrogen bonds.[28] In all cases, R_{A-B} decreases in the transition state. In addition, ∠AHB increases from the ground to the transition state, except for $N_2H_7^+$, in which the angle is 180° in both states. All the transition states have

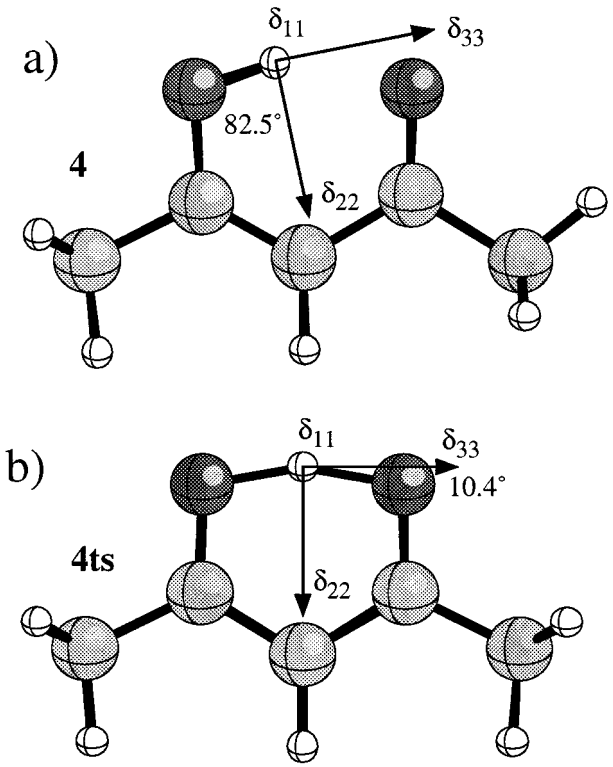

Figure 6. GIAO-MP2/tz2p chemical shift tensor orientation for **4** and **4ts**. Each molecule has at least a symmetry plane and thus the relative orientation of the tensor is determined by symmetry. One component (δ_{11} in each case here) lies perpendicular to the page, the other two lie in the plane of the page, and the angle between one component and the O−H bond vector is shown.

chemical shifts which are downfield (more positive) of the minimum energy structures. In most cases, the difference between the shift for the transition state and that for the ground state is only 1−2 ppm (for **2** it is 5.1 ppm). In **4**, the one case in this work in which the ground state might be considered a moderate rather than a strong hydrogen bond, the chemical shift of the transition state is 9.3 ppm farther downfield than the proton shift for the ground state. In agreement with other workers, we find that hydrogen atoms in strong hydrogen bonding environments have unusually downfield chemical shifts.[3,4] In the predicted structures of transition states for proton transfer, we find that the ^{1}H chemical shift is downfield of the corresponding ground state.[4] In addition, the CSA is always larger for the predicted transition state than for the corresponding ground state. This difference in CSA values, combined with the fact that the chemical shift for the transition states is consistently downfield of the associated ground state, supports the claim that the CSA may be useful as a measure of hydrogen bond strength.[3,49] Since we did not calculate hydrogen bonding energies in this work, we cannot comment further on this effect.

It has previously been suggested that the electron correlation contribution to the ^{1}H isotropic chemical shielding is generally small, ca. 0.2 ppm.[26] For conventional hydrogens, we obtain the same result. However, for hydrogens that are in moderate or strong hydrogen bonding environments, this is not the case. In the molecules studied here the GIAO-MP2 shieldings are consistently larger than the GIAO-RHF values by 0.3−1.7 ppm. When treated as shifts relative to TMS, this difference becomes 0.7−2.1 ppm because of the additional correlation effect in the calculation of TMS. Note that because of the change in sign between the scales for shieldings and shifts, the GIAO-MP2 shifts are upfield (less positive) of the GIAO-RHF shifts. It appears then that GIAO-RHF level calculations may not be sufficient for accurate calculations of hydrogen-bonded systems not only because the correlation contribution is reasonably large, but because it also varies from molecule to molecule by up to 1.4 ppm. Whereas it is well-known that the MP2 level of theory tends to somewhat overestimate correlation effects, the MP2 values likely represent the maximum effect of electron correlation. On the ^{1}H chemical shift scale, even an extended one that considers isotropic shifts as far downfield as 24 ppm, a 1.4 ppm correlation effect is significant. Most pertinent to our own interests, the significant and variable correlation effects observed here for conventional hydrogen bonding cases suggests that correlation needs to be included in ^{1}H shift calculations for hydrogen-bonded complexes in zeolites. While a similar conclusion was not unexpected for ^{13}C shifts of adsorbates in these same zeolite complexes, we had hoped that ^{1}H shifts of complexes formed on solid acids would generally be tractable at GIAO-RHF. Unfortunately, compared to the RHF level, the increased computational cost, memory, and disk requirements of MP2 shift calculations, similar to those of MP2 frequency calculations, make the MP2 treatment tractable for only relatively small systems, such as those studied here The present study then suggests the cautious application of ^{1}H shift calculations to problems in acid catalysis and underscores the need to develop computationally more efficient methods, such as DFT, for correlated chemical shift calculations. [52]

Summary and Conclusion

We calculated the minimum energy and transition-state geometries for several archetypal examples of hydrogen bonds, including structures with different charge and donor−acceptor atoms. We have calculated the chemical shift tensors at both the GIAO-RHF and GIAO-MP2 levels of theory. The donor acceptor distance R_{A-B} contracts in the transition state. Chemical shift calculations at the GIAO-RHF level consistently overestimate the GIAO-MP2 isotropic shift of the proton involved in the hydrogen bond. The discrepancy was ca. 1 ppm for moderate hydrogen bonds and ca. 2.0 ppm for strong hydrogen bonds. Electron correlation therefore has a strong effect on the ^{1}H chemical shifts of hydrogen bonds and must be included in order to obtain accurate results. Our chemical shift calculations are in reasonable agreement with experimental chemical shift tensor measurements. The proton shift for the transition states were invariably downfield of those for the corresponding minima. The chemical shift anisotropy, as well as the isotropic proton shift, changes with hydrogen bond strength.

Acknowledgment. J.F.H. is supported by the National Science Foundation (CHE-9996109) and the U.S. Department of Energy (DOE) Office of Basic Energy Sciences (BES) (Grant No. DE-FG03-93ER14354). J.B.N. was funded by the Department of Energy (DOE) Office of Science. Computer resources were provided by the National Energy Research Supercomputer Center (NERSC), Berkeley, CA, the Molecular Science Computing Facility (MSCF) at PNNL, and the National Center for Supercomputing Applications (NCSA). The MSCF is operated with funds provided by DOE's Office of Biological and Environmental Research. Pacific Northwest National Laboratory is a multipurpose national laboratory operated by Battelle Memorial Institute for the U.S. DOE.

Supporting Information Available: Eleven tables reporting theoretical geometries (5 pages). This material is available free of charge via the Internet at http://pubs.acs.org.

References and Notes

(1) Chen, J.; McAllister, M. A.; Lee, J. K.; Houk, K. N. *J. Org. Chem.* **1998**, *63*, 4611−4619.

(2) Kumar, G. A.; Pan, Y. P.; Smallwood, C. J.; McAllister, M. A. *J. Comput. Chem.* **1998**, *19*, 1345−1352.

(3) Garcia-Viloca, M.; Gelabert, R.; González-Lafont, A.; Moreno, M.; Lluch, J. M. *J. Phys. Chem. A* **1997**, *101*, 8727−8733.

(4) Garcia-Viloca, M.; Gonzáles-Lafont, A.; Lluch, J. M. *J. Am. Chem. Soc.* **1997**, *119*, 1081−1086.

(5) Pan, Y.; McAllister, M. A. *J. Am. Chem. Soc.* **1998**, *120*, 166−169.

(6) Smallwood, C. J.; McAllister, M. A. *J. Am. Chem. Soc.* **1997**, *119*, 11 277−11 281.

(7) Tuckerman, M. E.; Marx, D.; Klein, M. L.; Parrinello, M. *Science (Washington, D. C.)* **1997**, *275*, 817−820.

(8) Cleland, W. W.; Kreevoy, M. M. *Science (Washington, D. C.)* **1994**, *264*, 1887−1890.

(9) Del Bene, J. E.; Jordan, M. J. T. *J. Am. Chem. Soc.* **2000**, *122*, 4794−4797.

(10) Del Bene, J. E.; Perera, S. A.; Bartlett, R. J. *J. Phys. Chem. A* **1999**, *103*, 8121−8124.

(11) Garcia-Viloca, M.; Gelabert, R.; Gonzalez-Lafont, A.; Moreno, M.; Lluch, J. M. *J. Am. Chem. Soc.* **1998**, *120*, 10203−10209.

(12) Kulkarni, S. A. *J. Phys. Chem. A* **1998**, *102*, 7704−7711.

(13) Kumar, G. A.; Mcallister, M. A. *J. Org. Chem.* **1998**, *63*, 6968−6972.

(14) Scheiner, S.; Kar, T. *J. Am. Chem. Soc.* **1995**, *117*, 6970−6975.

(15) Warshel, A.; Papazyan, A.; Kollman, P. A. *Science (Washington, D. C.)* **1995**, *269*.

(16) Guthrie, J. P. *Chem. Biol.* **1996**, *3*, 163−170.

(17) Gerlt, J. A.; Kreevoy, M. M.; Cleland, W. W.; Frey, P. A. *Chem. Biol.* **1997**, *4*, 259−267.

(18) Frey, P. A.; Whitt, S. A.; Tobin, J. B. *Science (Washington, D. C.)* **1994**, *264*, 1927−1930.

(19) Emsley, J. *Chem. Soc. Rev* **1980**, *9*, 91−124.

(20) Hibbert, F.; Emsley, J. *Adv. Phys. Org. Chem.* **1990**, *26*, 255−379.

(21) Haw, J. F.; Nicholas, J. B.; Xu, T.; Beck, L. W.; Ferguson, D. B. *Acc. Chem. Res.* **1996**, *29*, 259−267.

(22) Haw, J. F.; Xu, T.; Nicholas, J. B.; Goguen, P. W. *Nature (London)* **1997**, *389*, 832−835.

(23) Ditchfield, R. *Mol. Phys.* **1974**, *27*, 789−807.

(24) Wolinski, K.; Hinton, J. F.; Pulay, P. *J. Am. Chem. Soc.* **1990**, *112*, 8251−8260.

(25) Gauss, J. *Chem. Phys. Lett.* **1992**, *191*, 614−620.

(26) Chesnut, D. B. *Chem. Phys.* **1997**, *214*, 73−79.

(27) Schiøtt, B.; Iversen, B. B.; Madsen, G. K. H.; Bruice, T. C. *J. Am. Chem. Soc.* **1998**, *120*, 12 117−12 124.

(28) Jeffrey, G. A. *An Introduction to Hydrogen Bonding*; Oxford University Press: New York, 1997.

(29) Becke, A. D. *J. Chem. Phys.* **1993**, *98*, 5648−5652.

(30) Lee, C.; Yang, W.; Parr, R. G. *Phys. Rev. B: Condens. Matter* **1988**, *37*, 785−789.

(31) Gordon, M. S. *Chem. Phys. Lett.* **1980**, *76*, 163.

(32) Møller, C.; Plesset, M. S. *Phys. Rev.* **1934**, *46*, 618−622.

(33) Hehre, W. J.; Radom, L.; Schleyer, P. v. R.; Pople, J. A. *Ab Initio Molecular Orbital Theory*; Wiley & Sons: New York, 1986.

(34) Kendall, R. A.; Dunning, T. H.; Harrison, R. J. *J. Chem. Phys.* **1992**, *96*, 6796−6806.

(35) Gaussian 94, Revision E.2. Frisch, M. J.; Trucks, G. W.; Schlegel, H. B.; Gill, P. M. W.; Johnson, B. G.; Robb, M. A.; Cheeseman, J. R.; T. Keith; Petersson, G. A.; Montgomery, J. A.; Raghavachari, K.; Al-Laham, M. A.; Zakrzewski, V. G.; Ortiz, J. V.; Foresman, J. B.; Cioslowski, J.; Stefanov, B. B.; Nanayakkara, A.; Challacombe, M.; Peng, C. Y.; Ayala, P. Y.; Chen, W.; Wong, M. W.; Andres, J. L.; Replogle, E. S.; Gomperts, R.; Martin, R. L.; Fox, D. J.; Binkley, J. S.; Defrees, D. J.; Baker, J.; Stewart, J. P.; Head-Gordon, M.; Gonzalez, C.; Pople, J. A.; Pittsburgh, PA, 1995.

(36) Schäfer, A.; Huber, C.; Ahlrichs, R. *J. Chem. Phys.* **1994**, *100*, 5829−5835.

(37) Stanton, J. F.; Gauss, J.; Watts, J. D.; Lauderdale, W. J.; Bartlett, R. J. *Int. J. Quantum Chem.* **1992**, *S26*, 879−894.

(38) Xu, T.; Torres, P. D.; Barich, D. H.; Nicholas, J. B.; Haw, J. F. *J. Am. Chem. Soc.* **1997**, *119*, 396−405.

(39) Duncan, T. M. *A Compilation of Chemical Shift Anisotropies*; Farragut Press: Chicago, 1990.

(40) Bozorth, R. M. *J. Am. Chem. Soc.* **1923**, *45*, 2128−2132.

(41) Van Hecke, P.; Spiess, H. W.; Haeberlen, U. *J. Magn. Reson.* **1976**, *22*, 103−116.

(42) Frisch, M. J.; Del Bene, J. E.; Binkley, J. S.; Schaefer, H. F., III *J. Chem. Phys.* **1986**, *84*, 2279−2280.

(43) Del Bene, J. E. *J. Comput. Chem.* **1989**, *10*, 603−615.

(44) Berthold, H. J.; Preibsch, W.; Vonholdt, E. *Angew. Chem., Int. Ed. Engl.* **1988**, *27*, 1524−1525.

(45) Iijima, K.; Ohnogi, A.; Shibata, S. *J. Mol. Struct.* **1987**, *156*, 111.

(46) Xu, T.; Barich, D. H.; Torres, P. D.; Haw, J. F. *J. Am. Chem. Soc.* **1997**, *119*, 406−414.

(47) Nicholas, J. B.; Xu, T.; Barich, D. H.; Torres, P. D.; Haw, J. F. *J. Am. Chem. Soc.* **1996**, *118*, 4202−4203.

(48) Lintvedt, R. L.; Holtzclaw Jr., H. F. *J. Am. Chem. Soc.* **1966**, *88*, 2713−2716.

(49) Ditchfield, R. *J. Chem. Phys.* **1976**, *65*, 3123−3133.

(50) Nicholas, J. B.; Xu, T.; Barich, D. H.; Torres, P. D.; Haw, J. F. *J. Am. Chem. Soc.* **1996**, *118*, 4202−4203.

(51) Hinton, J. F.; Guthrie, P.; Pulay, P.; Wolinski, K. *J. Am. Chem. Soc.* **1992**, *114*, 1604−1605.

(52) DFT NMR calculations for generally much less computationally expensive than MP2 calculations (for a given system) and offer an alternative means of studying NMR properties of large systems. See, for example: Rauhut, G.; Puyear, S.; Wolinski, K.; Pulay, P. *J. Phys. Chem.* **1996**, *100*, 6310−6316.